Chemosphere 311 (2023) 136994

Contents lists available at ScienceDirect

Chemosphere

journal homepage: www.elsevier.com/locate/chemosphere

Fungal necromass presents a high potential for Mercury immobilization in soil

François Maillard [a,*], Stéphane Pflender [b], Katherine A. Heckman [c], Michel Chalot [b,d], Peter G. Kennedy [a]

[a] Department of Plant & Microbiology, University of Minnesota, St. Paul, MN, 55108, USA
[b] UMR Chrono-Environnement, CNRS 6249, Université Bourgogne Franche-Comté, 25000, Besançon, France
[c] USDA Forest Service Northern Research Station, Houghton, MI, 49931, USA
[d] Faculté des Sciences et Technologies, Université de Lorraine, 54000, Nancy, France

HIGHLIGHTS

- Fungal necromass accumulates large quantities of Mercury (Hg) in soil.
- Hg biosorption depends on the chemical properties of fungal residues.
- Lipid acyl chains are positively related to Hg adsorption on fungal necromass.

GRAPHICAL ABSTRACT

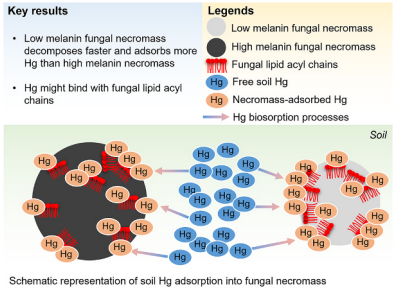

Schematic representation of soil Hg adsorption into fungal necromass

ARTICLE INFO

Handling Editor: T Cutright

Keywords:
Hg biosorption
Hg cycle
Fungal necromass
Phytostabilization

ABSTRACT

Past industrial activities have generated many contaminated lands from which Mercury (Hg) escapes, primarily by volatilization. Current phytomanagement techniques aim to limit Hg dispersion by increasing its stabilization in soil. Although soil fungi represent a source of Hg emission associated with biovolatilization mechanisms, there is limited knowledge about how dead fungal residues (i.e., fungal necromass) interact with soil Hg. This study determined the Hg biosorption potential of fungal necromass and the chemical drivers of passive Hg binding with dead mycelia. Fungal necromass was incubated under field conditions with contrasting chemical properties at a well-characterized Hg phytomanagement experimental site in France. After four months of incubation in soil, fungal residues passively accumulated substantial quantities of Hg in their recalcitrant fractions ranging from 400 to 4500 μg Hg/kg. In addition, infrared spectroscopy revealed that lipid compounds explained the amount of Hg biosorption to fungal necromass. Based on these findings, we propose that fungal necromass is likely an important factor in Hg immobilization in soil.

* Corresponding author. Gortner Avenue Saint Paul, MN, 55108, USA.
E-mail address: francois.maillard2@gmail.com (F. Maillard).

https://doi.org/10.1016/j.chemosphere.2022.136994
Received 16 August 2022; Received in revised form 17 October 2022; Accepted 21 October 2022
Available online 1 November 2022

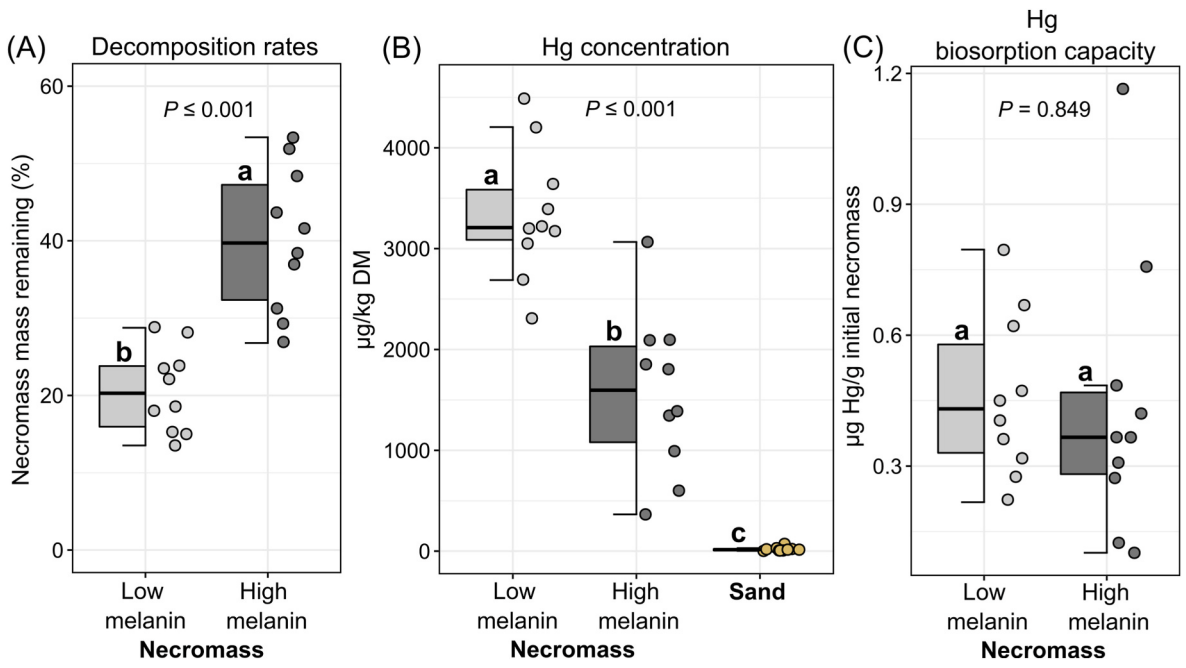

Fig. 1. (a) Fungal necromass remaining (% of initial dry mass) depending on necromass type (*i.e.,* low and high melanin). (b) Hg concentration (µg/kg dry mass) for fungal necromass (*i.e.*, low and high melanin necromasses) and silica sand. (b) For low and high melanin necromass types, Hg biosorption capacity (µg Hg/g of initial necromass). Fungal necromass remaining and Hg biosorption capacity were compared using Student's T-test. Differences in Hg concentrations in fungal necromass and silica sand were assessed using one-way ANOVA followed by Tukey's HSD test. Different letters denote significant differences ($P \leqslant 0.05$).

1. Introduction

Hg is a trace metal that accumulates within food chains and presents high toxicity for fauna and humans (Renzoni et al., 1998; Rice et al., 2014). As anthropogenic activities have drastically increased global Hg emissions, remediating the pollution associated with this trace metal has become an important challenge (Sundseth et al., 2017). Industrial activities have generated many contaminated soils from which Hg escapes through water runoff and volatilization, making Hg particularly difficult to contain compared with non-volatile trace metals (Kocman et al., 2013, 2017). Bioremediation has emerged as a viable alternative for managing polluted soils and, notably, phytoextraction, which consists of removing metals using hyperaccumulating plants (Marrugo-Negrete et al., 2015). Nevertheless, the restricted number of high biomass Hg-hyperaccumulating plants reduces the phytoextraction capacity for Hg (Rodriguez et al., 2005). As such, stabilizing Hg in soil has become the dominant research hypothesis for treating polluted sites by restricting Hg movement in the biosphere (Zgorelec et al., 2020). However, exactly how Hg is immobilized in soils remains poorly understood, mostly because of the complex biotic and abiotic interactions of Hg with soil organic matter and microorganisms (Barkay and Wagner-Dobler, 2005; Durand et al., 2020).

Soil fungi can accumulate large quantities of trace metals by biosorption when they are either alive or dead (Ayele et al., 2021). While Hg bioaccumulation in fungal fruit bodies (i.e. mushrooms) has received much attention, how the fungal mycelial structure that represents most of the fungal biomass in terrestrial ecosystems accumulates Hg has drawn very little study (Durand et al., 2020). Biosorption of Hg on fungal mycelial residues (i.e., fungal necromass) has been primarily described under laboratory conditions (Amin et al., 2016). Notably, fungal necromass passively and rapidly binds Hg from aqueous solutions (Martinez-Juarez et al., 2012). In parallel, recent studies have highlighted that residues originating from soil fungi contribute to a large proportion of soil organic matter by representing up to 50% of the stabilized soil carbon (Angst et al., 2021; Wang et al., 2021a, 2021b). It has consistently been found that fungal necromass decomposes extremely fast until it reaches a plateau phase, generally corresponding to 10–20% of mass remaining, which strongly correlates with initial necromass melanin content, a pigment found in ~2/3 of soil fungi (Siletti et al., 2017; Fernandez and Kennedy, 2018; Fernandez et al., 2019; See et al., 2021). Also, the recalcitrant fraction of fungal residues can persist for years in soils without apparent signs of decomposition (Maillard et al., 2021). Taken together, the Hg biosorption of fungal necromass and its high recalcitrance suggest that fungal necromass might be capable of significant Hg sequestration in polluted soils. However, the biosorption of Hg on fungal necromass has been mostly investigated to produce filters to remove Hg from aqueous solutions (Martinez-Juarez et al., 2012; Amin et al., 2016). Consequently, we lack studies demonstrating Hg biosorption in mycelial residues in soil as well as identifying the intrinsic chemical properties of fungal necromass that facilitate passive Hg binding.

We aimed to test whether fungal necromass sequestrated Hg in its recalcitrant fraction (i.e., the portion of mass remaining following a period of incubation in soil). Thus, we incubated fungal necromass presenting contrasted chemical composition (i.e., differences in melanin content) in the soil of a well-characterized Hg-contaminated site. Given that Hg adsorbance on fungal necromass has been described in aqueous solutions in-vitro, we speculated that fungal residues would also accumulate Hg when incubated in soil. Additionally, we hypothesized that highly melanized necromass would accumulate more Hg because of melanin's trace metal scavenging properties (Rizzo et al., 1992; Manirethan et al., 2018).

2. Materials and methods

We produced fungal necromass from *Meliniomyces bicolor* (*Meliniomyces* PMI_1271; see https://mycocosm.jgi.doe.gov/MelPMI1271_1/MelPMI1271_1.home.html for more information about the strain used in the present study), a widely distributed soil fungus establishing mutualistic interactions with tree species, with contrasting chemical morphologies based on the protocol described in Fernandez and Kennedy (2018). The melanization levels in *M. bicolor* were

Table 1
Summary of the identified FTIR peaks, their putative functional group, averaged absorbance depending on necromass type (i.e., low and high melanin) before and post incubation, and their Pearson's correlation coefficient and significance when correlated with necromass Hg concentration. Differences in selected peaks absorbance were assessed using one-way ANOVA followed by Tukey's HSD test. Different letters denote significant differences ($P \leqslant 0.05$).

Peak number	Frequency (cm^{-1})	Functional group	Initial necromass: low melanin	Initial necromass: high melanin	Incubated necromass: low melanin	Incubated necromass: high melanin	Pearson's coefficient with necromass [Hg]	Pearson's P
1	3360	(O–H)	3.58 ± 0.32 a	3.57 ± 0.07 a	3.37 ± 0.1 a	3.43 ± 0.02 a	−0.11	0.63
2	2924	Aliphatic (C–H)	**2.74 ± ;0.11 a**	**2.59 ± ;0.03 a**	**1.94 ± ;0.07 b**	**1.88 ± ;0.02 b**	0.02	0.93
3	2850	Aliphatic (C–H)	**1.76 ± ;0.14 a**	**1.74 ± ;0.02 a**	**1.36 ± ;0.04 b**	**1.44 ± ;0.02 b**	**−0.5**	**0.026**
4	1650	Amide (N–H)	2.72 ± 0.21 a	2.59 ± 0.09 a	2.5 ± 0.1 a	2.51 ± 0.03 a	0.04	0.88
5	1540	Amide (C=O)	1.67 ± 0.22 a	1.52 ± 0.06 a	1.73 ± 0.09 a	1.79 ± 0.03 a	−0.09	0.7
6	1425	Aromatic (C=C)	1.39 ± 0.12 a	1.47 ± 0.02 a	2.64 ± 0.35 a	2.35 ± 0.16 a	0.25	0.28
7	1385	Aliphatic (C–H)	1.87 ± 0.12 a	1.76 ± 0.04 a	2.57 ± 0.22 a	2.27 ± 0.11 a	0.35	0.13
8	1250	Aromatic (C–O)	1.43 ± 0.15 a	1.34 ± 0.02 a	1.27 ± 0.04 a	1.3 ± 0.01 a	−0.16	0.49
9	1160	Polysaccharide (C–O)	**1.99 ± ;0.08 a**	**1.94 ± ;0.01 a**	**1.8 ± ;0.09 a**	**1.53 ± ;0.01 b**	0.43	0.059
10	1075	Polysaccharide (C–O)	**3.55 ± ;0.26 a**	**3.75 ± ;0.14 a**	**3.16 ± ;0.08 b**	**2.97 ± ;0.03 b**	0.39	0.085
11	1040	(C–O, C–C)	**3.38 ± ;0.29 a**	**3.56 ± ;0.12 a**	**3.19 ± ;0.07 ab**	**2.99 ± ;0.03 b**	0.41	0.07
12	877	Aromatic (C–H)	0.31 ± 0.02 a	0.3 ± 0.03 a	0.63 ± 0.13 a	0.39 ± 0.06 a	0.44	0.054
13	715	Aliphatic (C–H)	**0.59 ± ;0.03 a**	**0.58 ± ;0.01 a**	**0.59 ± ;0.02 a**	**0.39 ± ;0.02 b**	**0.9**	**0.000001**

modified by growing mycelial plugs in 125 ml flasks with different levels of submersion (i.e., respectively 40 or 120 ml for lowly or highly melanized biomass) in half-strength potato dextrose broth (PDB, Difco, BD Products, Franklin Lakes, New Jersey, USA). After 30 days of incubation on orbital shakers at 150 RPM at room temperature, the two forms of *M. bicolor* residues differing primarily in melanin content, hereafter referred to as low and high melanin *M. bicolor* necromass , were harvested, rinsed with autoclaved deionized water, and freeze-dried. Mesh bags (with 53-μm pores) containing 140 mg of low or high melanin necromass (*i.e.,* mycobags) were buried in the top 10 cm of soil at a Hg-contaminated phytomanagement site in France planted with *Populus* trees (n = 10 mycobags for each necromass type) and having a soil Hg concentration around 6000 μg Hg/kg (Maillard et al., 2016; Yung et al., 2019). For reference 60 μg Hg/kg was the average background concentration of Hg in non-contaminated soils (Wang et al., 2012; Amos et al., 2013). An additional set of bags were made with silica sand to control for potential contamination by soil particles (i.e., sandbag, n = 10) and buried within 50 cm of the mycobags. After four months of incubation from May to September 2021, mesh bags were harvested, and fungal necromasses and sands were air dried. We then measured the decomposition rates of the two necromass types. Total Hg for fungal necromass and sand was analyzed using an AMA254 Mercury Analyzer, as described in Maillard et al. (2016). Fourier-transform infrared spectroscopy (FTIR) was applied to characterize the chemical properties of the initial and remaining fungal necromass, as outlined in Fernandez et al. (2019). Based on the literature, the observed FTIR peaks were assigned to functional chemical groups (Fernandez et al., 2019; Dzurendova et al., 2020; Langseter et al., 2021). Finally, using Pearson's correlations, we tested the relationships between fungal necromass Hg concentration and FTIR profile of both necromass types to identify the main compounds responsible for Hg adsorption onto dead fungal hyphae.

3. Results and discussion

After four months of incubation in soil, the mesh bags were harvested and checked for integrity. Two sandbags with clear root penetration were excluded from the analyses. We found a significant effect of necromass type on the decomposition rates, with approximately twice the mass remaining for the high melanin fungal necromass by comparison with the low melanin type ($P \leqslant 0.001$) (Fig. 1a). Based on FTIR profiling, remaining necromass of both types was significantly depleted ($P \leqslant 0.05$) in aliphatic compounds and polysaccharides and tended to be enriched in aromatic molecules by comparison with initial fungal residues (Table 1). These results paralleled those of Fernandez and Kennedy (2018) and Ryan et al. (2020), who both described similar differences in decomposition trajectories and chemical evolution for low and high melanized *Meliniomyces* necromass. More generally, our results align with the fact that a large fraction of fungal residues is resistant to decomposition and might persist in a particulate form for long time periods in soils (Fernandez et al., 2019; Maillard et al., 2021). Before incubation, we measured 15 and 11 μg Hg/kg of dry mass for the low and high melanin necromass types, respectively, indicating no initial Hg enrichment of the fungal residues during the necromass production process (Durand et al., 2020). In addition, we quantified 15 μg Hg/kg of dry mass for the silica sand incubated in parallel to the mycobags, confirming that no substantial soil contamination of the mesh bags occurred throughout the experiment. The Hg concentrations detected in fungal necromass ranged from 400 to 4500 μg Hg/kg (Fig. 1b) and were high regarding the soil Hg concentration at our experimental site, around 6000 μg Hg/kg (Yung et al., 2019). However, it has been shown that fungal residues might accumulate up to 20,000 more Hg in laboratory experiments (*e.g.*, 30–70 mg Hg/g of fungal necromass) than what we observed in our field study (Say et al., 2003; Amin et al., 2016). As such, soil Hg concentration and bioavailability, not necromass total adsorption capacity, were likely to be the limiting factors of Hg

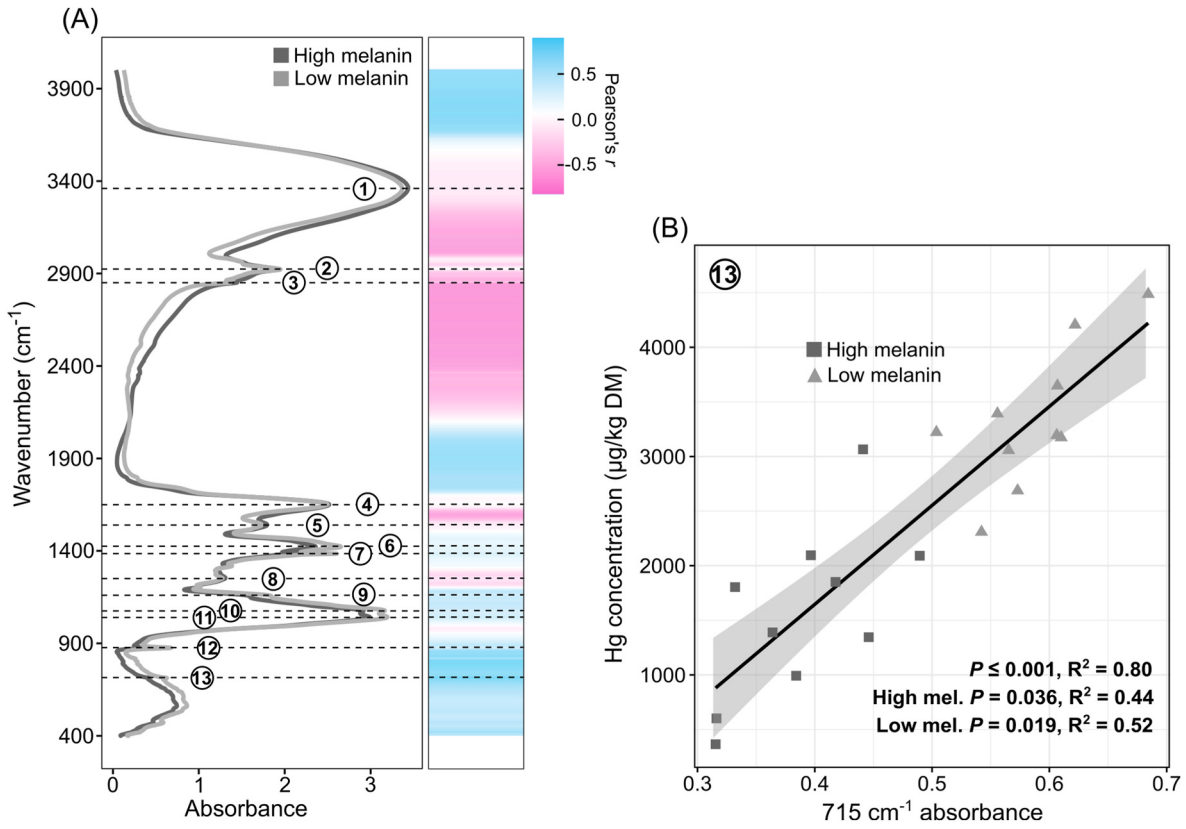

Fig. 2. **(a)** Averaged FTIR profiles for low and high melanin necromass types post incubation. The numbers in circles represent the identified peaks (Table 1). Insert on the left side of the figure displays Pearson's correlations between necromass FTIR data (cm^{-1}) and Hg concentration (µg/kg dry mass). (b) Pearson's correlations between peak 15 (715 cm^{-1}) and Hg concentration (µg/kg dry mass) for the two necromass types together and separately.

sequestration in our experimental conditions. Longer incubations would be essential to assess if fungal necromass keeps accumulating Hg with time as well as if Hg desorption from necromass might also occur.

Hg concentrations varied by necromass type, with the low melanin type being significantly more than twice as enriched in Hg compared to high melanin necromass ($P \leqslant 0.001$) (Fig. 1b). These results contradicted our hypothesis about the role of melanin in Hg biosorption and revealed that other fungal necromass compounds were responsible for passive Hg binding. However, given that the low melanin necromass had a faster decomposition rate but accumulated more Hg than high melanin necromass, Hg biosorption potential was not significantly different between the two necromass types (Fig. 1c). Post-incubation FTIR profiling also displayed very similar chemical profiles for the remaining fractions of the low and high melanin necromasses (Fig. 2a, Table 1). This indicates that after the labile portion of necromass decomposed, the chemical composition of the remaining recalcitrant fractions was very similar between the two studied necromass types. It was not surprising given that the same fungal species was used to produce the two types of necromass residues. Hg concentration in fungal necromass was significantly positively correlated with peak 13 (715 cm^{-1}), explaining up to 80% of Hg adsorption for the two necromass types together and 44% and 52%, respectively, for the high and low melanin necromass types when analyzed separately (Fig. 2b). Infrared peaks at an absorbance of 715–720 cm^{-1} have already been described for soil fungi and are associated with lipid acyl chains (Kosa et al., 2017; Langseter et al., 2021). Consequently, our results suggest that lipid acyl chains might play a key role in passive Hg binding to fungal necromass. Further necromass chemical characterization is needed to confirm the roles of fungal lipids in Hg adsorption by necromass, notably by fractionating fungal molecules and testing for their respective Hg sorption under laboratory conditions.

Our study demonstrates that dead mycelial residues present in soil can passively adsorb substantial quantities of Hg under field conditions. Given the large production of soil fungal biomass in combination with the rapid turnover of fungal hyphae (See et al., 2022), fungal necromass is likely the primary source of soil organic matter in newly restored and replanted contaminated soils. Thus, fungal necromass production might explain why vegetated polluted areas emit less gaseous Hg than non-vegetated soils (Stamenkovic et al., 2008; Fantozzi et al., 2013). Our results also confirm the role of soil organic matter in limiting Hg mobility in soil (Yin et al., 1996, 1997; Liu et al., 2018; Johs et al., 2019). In contrast to remediation techniques based on the addition of chemical sorbents, fungal necromass production is a naturally occurring process in the soil that might be enhanced to improve Hg immobilization (Ahmad et al., 2014; Wang et al., 2021b). For example, polluted sites could be restored with plants harboring fungal consortia producing high biomass and having high chemical-Hg-binding properties. Regardless, while our study is among the first to assess the roles of fungal necromass in Hg cycling, we still have limited knowledge about the roles of fungi in Hg cycling and speciation while they are alive. For example, it has been depicted that fungi can internalized Hg (Durand et al., 2020) and generate Hg-based volatiles (Urík et al., 2014; Kodre et al., 2017). Thus, promoting fungal biomass production might increase Hg biovolatilization. Additionally, fungal residues also represent a food source for soil fauna, and as a potential consequence, increasing fungal necromass formation could intensify the Hg bioaccumulation phenomenon observed within terrestrial food chains (Yung et al., 2019).

4. Conclusions

In conclusion, we show that fungal residues present in soil passively adsorbed substantial quantities of Hg. Furthermore, Hg accumulation in

fungal necromass varied depending on the chemical properties of necromass and was strongly associated with lipid compounds. We propose that fungal necromass might play a central role in the Hg global cycle. More holistic studies, including the impact on Hg cycling of both living and dead fungal components, are necessary to measure the net effect of these ubiquitous microorganisms on Hg emission from soil.

Author's contributions

F.M. coordinated the project. F.M., K.A.H., M.C., and P.G.K. designed the study. F.M., S.P., K.A.H., and M.C. carried out the experiments and performed the data analyses. F.M., S.P., K.A.H., M.C., and P.G.K. interpreted the data. F.M. wrote the manuscript with help from K.A.H., M.C., and P.G.K.

Declaration of competing interest

The authors declare that they have no known competing financial interests or personal relationships that could have appeared to influence the work reported in this paper.

Data availability

Data will be made available on request.

Acknowledgements

We thank the two reviewers for their helpful comments on our manuscript. The authors also thank the U.S. National Science Foundation (#DEB 2038293) and the French ANR (#2010-INTB- 1703-03 BIOFILTREE) for financial support. Finally, we also thank the Genomic Science Program (U.S. Department of Energy) Plant Microbe Interfaces (PMI) Scientific Focus Area (http://pmi.ornl.gov/) for providing the *Meliniomyces* strain used in this study.

References

Ahmad, M., Rajapaksha, A.U., Lim, J.E., Zhang, M., Bolan, N., Mohan, D., et al., 2014. Biochar as a sorbent for contaminant management in soil and water: a review. Chemosphere 99, 19–33.

Angst, G., Mueller, K.E., Nierop, K.G.J., Simpson, M.J., 2021. Plant- or microbial-derived? A review on the molecular composition of stabilized soil organic matter. Soil Biol. Biochem. 156, 108189.

Amin, F., Talpur, F.N., Balouch, A., Chandio, Z.A., Surhio, M.A., Afridi, H.I., 2016. Biosorption of mercury (II) from aqueous solution by fungal biomass *Pleurotus eryngii*: isotherm, kinetic, and thermodynamic studies. Environ. Prog. Sustain. Energy 35 (5), 1274–1282.

Amos, H.M., Jacob, D.J., Streets, D.G., Sunderland, E.M., 2013. Legacy impacts of all-time anthropogenic emissions on the global mercury cycle. Global Biogeochem. Cycles 27, 410–421.

Ayele, A., Haile, S., Alemu, D., Kamaraj, M., 2021. Comparative utilization of dead and live fungal biomass for the removal of heavy metal: a concise review. Sci. World J. Article ID 5588111, 10 pages.

Barkay, T., Wagner-Dobler, I., 2005. Microbial transformations of mercury: potentials, challenges, and achievements in controlling mercury toxicity in the environment. Adv. Appl. Microbiol. 57, 1–52.

Durand, A., Maillard, F., Foulon, J., et al., 2020. Interactions between Hg and soil microbes: microbial diversity and mechanisms, with an emphasis on fungal processes. Appl. Microbiol. Biotechnol. 104, 9855–9876.

Dzurendova, S., Zimmermann, B., Kohler, A., Tafintseva, V., Slany, O., Certik, M., Shapaval, V., 2020. Microcultivation and FTIR spectroscopy-based screening revealed a nutrient-induced co-production of high-value metabolites in oleaginous Mucoromycota fungi. PLoS One 15, e0234870.

Fantozzi, L., Ferrara, R., Dini, F., Tamburello, L., Pirrone, N., Sprovieri, F., 2013. Study on the reduction of atmospheric mercury emissions from mine waste enriched soils through native grass cover in the Mt. Amiata region of Italy. Environ. Res. 125, 69–74.

Fernandez, C.W., Heckman, K., Kolka, R., Kennedy, P.G., 2019. Melanin mitigates the accelerated decay of mycorrhizal necromass with peatland warming. Ecol. Lett. 22, 498–505.

Fernandez, C.W., Kennedy, P.G., 2018. Melanization of mycorrhizal fungal necromass structures microbial decomposer communities. J. Ecol. 106, 468–479.

Johs, A., Eller, V.A., Mehlhorn, T.L., Brooks, S.C., Harper, D.P., Mayes, M.A., et al., 2019. Dissolved organic matter reduces the effectiveness of sorbents for mercury removal. Sci. Total Environ. 690, 410–416.

Kodre, A., Arcon, I., Debeljak, M., Potisek, M., Likar, M., Vogel-Mikuš, K., 2017. Arbuscular mycorrhizal fungi alter Hg root uptake and ligand environment as studied by X-ray absorption fine structure. Environ. Exp. Bot. 133, 12–23.

Kocman, D., Horvat, M., Pirrone, N., Cinnirella, S., 2013. Contribution of contaminated sites to the global mercury budget. Environ. Res. 125, 160–170.

Kocman, D., Wilson, S.J., Amos, H.M., Telmer, K.H., Steenhuisen, F., Sunderland, E.M., et al., 2017. Toward an assessment of the global inventory of present-day mercury releases to freshwater environments. Int. J. Environ. Res. Publ. Health 14.

Kosa, G., Kohler, A., Tafintseva, V., Zimmermann, B., Forfang, K., Afseth, N.K., Tzimorotas, D., Vuoristo, K.S., Horn, S.J., Mounier, J., et al., 2017. Microtiter plate cultivation of oleaginous fungi and monitoring of lipogenesis by high-throughput FTIR spectroscopy. Microb. Cell Factories 1–12.

Langseter, A.M., Dzurendova, S., Shapaval, V., et al., 2021. Evaluation and optimization of direct transesterification methods for the assessment of lipid accumulation in oleaginous filamentous fungi. Microb. Cell Factories 20, 59.

Liu, P., Ptacek, C.J., Blowes, D.W., 2018. Mercury complexation with dissolved organic matter released from thirty-six types of biochar. Bull. Environ. Contam. Toxicol. 1, 6.

Maillard, F., Girardclos, O., Assad, M., Zappelini, C., Perez' Mena, J.M., Yung, L., Guyeux, C., Chretien, S., Bigham, G., Cosio, C., 'Chalot, M., 2016. Dendrochemical assessment of mercury releases from a pond and dredged-sediment landfill impacted by a chlor-alkali plant. Environ. Res. 148, 122–126.

Maillard, F., Kennedy, P.G., Adamczyk, B., et al., 2021. Root presence modifies the long-term decomposition dynamics of fungal necromass and the associated microbial communities in a boreal forest. Mol. Ecol. 30, 1921–1935.

Manirethan, V., Raval, K., Rajan, R., Thaira, H., Balakrishnan, R.M., 2018. Kinetic and thermodynamic studies on the adsorption of heavy metals from aqueous solution by melanin nanopigment obtained from marine source: *Pseudomonas stutzeri*. J. Environ. Manag. 214, 315–324.

Martinez-Juarez, V.M., Cardenas-Gonzalez, J.F., TorreBouscoulet, M.E., Acosta-Rodriguez, I., 2012. Biosorption of mercury(II) from aqueous solutions onto fungal biomass. Bioinorgan. Chem. Appl. 1. –5.

Marrugo-Negrete, J., Durango-Hernández, J., Pinedo-Hernández, J., Olivero-Verbel, J., Díez, S., 2015. Phytoremediation of mercury-contaminated soils by *Jatropha curcas*. Chemosphere 127, 58–63.

Ryan, M.E., Schreiner, K.M., Swenson, J.T., Gagne, J., Kennedy, P.G., 2020. Rapid changes in the chemical composition of degrading ectomycorrhizal fungal necromass. Fungal Ecol 45, 100922.

Renzoni, A.F., Ziet, A.F., Franchi, E., 1998. Mercury levels along the food chain and risk for exposed population. Environ. Res. 11, 68–72.

Rice, K.M., Walker, E.M., Wu, M., Gillette, C., Blough, E.R., 2014. Environmental mercury and its toxic effects. J. Prev. Med. Public Health. 47, 74–83.

Rizzo, D., Blanchette, R., Palmer, M., 1992. Biosorption of metal ions by Armillaria rhizomorphus. Can. J. Bot. Rev. 70, 1515–1520.

Rodriguez, L., Lopez-Bellido, F.J., Carnicer, A., Recreo, F., Tallos, A., Monteagudo, J.M., 2005. Mercury recovery from soils by phytoremediation. In: Lichtfouse, E., Schwarzbauer, J., Robert, D. (Eds.), Environmental Chemistry. Springer, pp. 197–204.

Say, R., Yilmaz, N., Denizli, A., 2003. Biosorption of cadmium, lead, mercury and arsenic ions by the fungus *Penicillium purpurogenum*. Separ. Sci. Technol. 38, 2039–2053.

See, C.R., Keller, A.B., Hobbie, S.E., Kennedy, P.G., Weber, P.K., Pett-Ridge, J., 2022. Hyphae move matter and microbes to mineral microsites: integrating the hyphosphere into conceptual models of soil organic matter stabilization. Global Change Biol.

Stamenkovic, J., Gustin, M.S., Arnone, J.A., Johnson, D.W., Larsen, J.D., Verburg, P.S.J., 2008. Atmospheric mercury exchange with a tallgrass prairie ecosystem housed in mesocosms. Sci. Total Environ. 406, 227–238.

Sundseth, K., Pacyna, J.M., Pacyna, E.G., Pirrone, N., Thorne, R.J., 2017. Global sources and pathways of mercury in the context of human health. Int. J. Environ. Res. Publ. Health 14, 105.

Siletti, C.E., Zeiner, C.A., Bhatnagar, J.M., 2017. Distributions of fungal melanin across species and soils. Soil Biol. Biochem. 113, 285–293.

Urík, M., Hlodák, M., Mikušová, P., et al., 2014. Potential of microscopic fungi isolated from mercury contaminated soils to accumulate and volatilize mercury(II). Water Air Soil Pollut. 225, 2219.

Wang, B., An, S., Liang, C., Liu, Y., Kuzyakov, Y., 2021a. Microbial necromass as the source of soil organic carbon in global ecosystems. Soil Biol. Biochem. 162.

Wang, J., Feng, X., Anderson, C.W., Xing, Y., Shang, L., 2012. Remediation of mercury contaminated sites–a review. J. Hazard Mater. 221, 1–18.

Wang, Y.J., Zhang, Y., Ok, Y.S., Jiang, T., Liu, P., Shu, R., Wang, D.Y., Cao, X.D., Zhong, H., 2021b. Biochar-impacted sulfur cycling affects methylmercury phytoavailability in soils under different redox conditions. J. Hazard Mater. 407, 124397.

Yin, Y., Allen, H.E., Li, Y., Huang, C.P., Sanders, P.F., 1996. Adsorption of mercury (II) by soil: effects of pH, chloride, and organic matter. J. Environ. Qual. 25, 837–844.

Yin, Y., Allen, H.E., Huang, C.P., Sanders, P.F., 1997. Adsorption/desorption isotherms of Hg (II) by soil. Soil Sci. 162, 35–45.

Yung, L., Bertheau, C., Cazaux, D., Regier, N., Slaveykova, V.I., Chalot, M., 2019. Insect life traits are key factors in mercury accumulation and transfer within the terrestrial food web. Environ. Sci. Technol. 53, 11122–11132.

Zgorelec, Z., Bilandzija, N., Knez, K., Galic, M., Zuzul, S., 2020. Cadmium and mercury phytostabilization from soil using *Miscanthus* × *giganteus*. Sci. Rep. 10.